Materials Physics and Mechanics 47 (2021) 681-696
Research article

Received: July 19, 2021
Accepted: November 1, 2021

AXIAL COMPRESSION BEHAVIOR OF THIN-WALLED MILD STEEL TUBES SUBJECTED TO AXIAL IMPACT

S.K. Tak✉, M.A. Iqbal

Indian Institute of Technology Roorkee, Roorkee, India

✉ sanjay.tak81@gmail.com

Abstract. The finite element computations were performed on ABAQUS/Explicit solver to study the effect of wall thickness on axial crushing and energy absorption of the mild steel tubes under axial impact. Circular tube (60 mm diameter) and square tube (47.34 mm size) with varying wall thicknesses (1.1, 1.5, 2, 2.5, and 3 mm) were impacted axially by 5 kg projectile. A comparative study has also been carried out on axial compression behavior of tubes with circular and square tubes with equivalent section areas. The constitutive and damage behavior of the mild steel was modelled using the Johnson-Cook material model. The validation of the computational model was carried out by performing the experiments on 60 mm diameter circular tube under the axial impact of 5 kg projectile. The maximum axial compression of the circular and square tubes has been found to be decreased with an increase in the wall thickness of the tubes, however, the absorbed energy does not show any significant influence with the change in the wall thickness of the tubes. The maximum axial compression of the square tubes was found to be higher than the circular tubes for thicknesses 1.1 and 1.5 mm. On the other hand, the axial compression of the circular tubes was found higher at higher thicknesses beyond 1.5 mm.

Keywords: axial deformation, energy absorber, crashworthiness, thin-walled tubes

Acknowledgements. *The first author acknowledges All India Council for Technical Education (AICTE) and Q.I.P. Centre, Indian Institute of Technology Roorkee, for providing the scholarship for his doctoral studies at the I.I.T. Roorkee, Roorkee, India. First author is also thankful to Institute computer centre, I.I.T. Roorkee, for providing the computational facilities.*

Citation: Tak S.K., Iqbal M.A. Axial compression behavior of thin-walled mild steel tubes subjected to axial impact // Materials Physics and Mechanics. 2021, V. 47. N. 5. P. 681-696. DOI: 10.18149/MPM.4752021_3.

1. Introduction

The safety of drivers and passengers is of utmost priority in automotive structures. Therefore, crashworthiness criteria should be considered in the design of such vehicles. Many researchers have suggested that energy absorber elements can be used to mitigate these impact problems. By the use of such energy-absorbing elements, structural deformations are ensured and crash energy is converted into strain energy for safety. Nowadays, thin-walled metal tubes are the most popular energy absorbers in different industries due to their ease of construction, crashworthiness, lighter weight, and economic significance. The axial dynamic compression behavior of uniform thickness, functionally graded thickness, and stepped thickness tubes under axial impact was studied experimentally and numerically [1]. It was

http://dx.doi.org/10.18149/MPM.4752021_3

reported that functionally graded thickness and stepped thickness steel tubes absorbed the same energy with less peak load and more axial shortening in comparison with the uniform thickness steel tubes. The axisymmetric buckling behavior of circular cylindrical shells studied numerically using an elastic-plastic material model with linear strain hardening concluded that the dynamic buckling mechanism is governed by the stress wave propagation [2]. It was found that the geometry of the shell and properties of the striker was the governing factor of the final buckling shapes. It was further reported that a low-velocity impact by a larger mass causes a significant bending deformation near the impacted end which causes progressive folding. On the other hand, a smaller mass-higher velocity impact may lead to a larger bending near the stationary end and a larger axial deformation near the impacted end [2]. The axial quasi-static compression behavior of aluminum tubes of 1 and 1.5 mm thicknesses with different cross-sections (triangular, rectangular, square, hexagonal, circular, pyramidal, and conical) was studied experimentally and numerically [3]. The triangular and circular sections absorbed the least and the most amount of energy among the all tested cross-sections respectively. A gradual increase in the cross-sectional area of the specimen affected the energy absorption as well as the average and the maximum force [3]. The energy absorption characteristics of the straight and tapered circular tubes with a graded thickness (TCTGT) were investigated under the axial loading leading to the conclusion that due to the larger design domain and better designability, the tapered tubes show better crashworthiness performance than the straight tubes [4].The performance in terms of energy absorption efficiency of functionally graded thickness (FGT) tubes with varying wall thickness had been significantly improved by optimizing the geometrical parameters and gradient exponent. It was also suggested that the thin-walled structures with variable thickness can be appropriate structures for innovative applications that require lightweight and high energy absorption [5]. Crashworthiness performance of conical tubes with various thickness distributions was investigated experimentally and numerically, showing the increment in material hardening during shrinking which is the key factor for the improvement of crashworthiness performance [6]. The crushing and energy absorption behavior of different windowed tubes were also studied under axial dynamic loading conditions. It was found that the circular tube with a square window shape reveals the best energy absorption characteristics [7]. The thin-walled tubes with an even number of sides have been the focused of many literatures. Meanwhile, little attention has been paid to the axial crushing of polygonal tubes with an odd number of sides, such as triangular tubes [8]. The triangular cross-section has exhibited the least energy absorbing capacity among all other tubes. In order to make improvements in the crashworthiness behavior of energy-absorbing structures, several arrangements of thin-walled profiles have been investigated, including single [9] and multi-cell [10]. Recently, a third category of thin-walled tubular structure called bi-tubular arrangement is emerging. These kinds of structures are formed by two concentric profiles with the same or different cross-sections. Several studies have been carried out to study bi-tubular structures. The crushing of monotubal and bi-tubular tubes under the axial loading was studied experimentally and numerically [11]. The absorbed energy and specific energy of combined bi-tubular tube were found higher than those of monotubal square or circular tubes designs. The crashworthiness analysis of double section bi-tubular thin-walled structures consisting of an inner tube with a different polygonal section such as triangle, square, or hexagon and an outer circular cylinder was studied under quasi-static axial compression leading to the conclusion that the bi-tubular stainless steel structures with hexagonal inner tube have more energy absorption capacity than the single-cylinder and the other bi-tube combinations [12]. The polynomial response surface models of single-cell and multi-cell square structures under axial loads were investigated to study the crashworthiness [13]. By taking the amplitude factor and eccentricity factor into account, a detailed theoretical

derivation of corrugated tubes under dynamic impacting [14] and quasi-static axial loading [15] had been presented. The axial and oblique crushing behavior of circular tubes with an externally press-fitted ring around the outer tube surface made from A36 steel hot rolled carbon were investigated numerically using the ABAQUS/explicit finite element solver [16]. It was proved that the ribbed tubes had better performance under axial and oblique impact compared with the conventional circular tubes. Compared with other unconventional tubular energy absorbing elements, the grooved tubes also have exceptional energy absorption performance, and easy processing is its obvious advantage [17]. The variation in the inner part, while keeping the outer part circular, of a bi-tubular structure under axial and oblique loading conditions was studied [18]. Apart from the configuration of bi-tubular structures, the effect of foam filler was also considered. The obtained results exhibited that bi-tubular structures were preferable under oblique loading conditions [18]. In addition to the aforementioned studies, the effect of the number of tubes made of AA-6101 and placed coaxially was examined under quasi-static axial load [19]. The results implied that specific energy absorption (SEA) and crash force efficiency (CFE) increased compared with those of monolithic structures with the same thickness, height, and mass. The distance between multi-wall tubular structures played an important role in the overall deformation characteristics. In this context, the crushing behavior of square, circular and hexagonal bi-tubular structures in terms of the radial clearance with cutouts as the crush initiators were also discussed [20]. The crashworthiness of axially varying thickness lateral corrugated tube (AVTLCT) under axial impact has been systematically studied using the verified finite element model [21]. It was found that the AVTLCT has great advantages in reducing the peak crushing force (PCF) and improving energy absorption. The finite element computations have been performed to study the quasi-static and dynamic axial compression behavior of circular and square mild steel tubes [22]. The behavior of both geometric sections was studied under different sizes and the response of the two equivalent sizes with different geometries was also compared. The axial deformation of both geometric sections decreased with the increase in the size under the dynamic and quasi-static loading conditions. The absorbed energy, on the other hand, did not show any significant influence on the size of the tube. The axial crushing of the tubes with square sections was found to be higher than the equivalent circular section [22]. Due to the excellent behaviors of energy absorbing performance and machining, thin-walled structures are widely used as energy absorbers. From the material point of view, the thin-walled energy absorbers can be made of fiber-reinforced composites (FRCs) and metallic materials [23]. Therefore, the thin-walled metallic tubular structures have attracted more attention in recent years because of their simple forms and excellent crashworthiness [23].

The majority of the research studies have been focused on the quasi-static performance of thin-walled metallic tubes while the dynamic behavior has not been effectively explored. The present study addresses the influence of wall thickness on axial crushing and energy absorption of thin-walled mild steel tubes subjected to projectile impact. An investigation of the dynamic performance of thin mild steel tubes has been carried out in this study to understand the axial deformation of circular and square tubes through nonlinear numerical simulations performed on ABAQUS/Explicit. A validation study of the computational model has been also presented wherein the axial performance of the thin-walled mild steel tubes of diameter 60 mm subjected to axial impact has been studied experimentally and FE simulations have been carried out for reproducing the actual results.

2. Numerical simulations

The three-dimensional models of thin-walled circular tubes of diameter 60 mm and square tubes of edge length 47.34 mm with 200 mm length and wall thicknesses (1.1,1.5, 2, 2.5, and 3 mm) were made in ABAQUS/CAE to study the influence of wall thickness on axial

deformation (compression) and energy absorption. The cylinder-shaped projectiles of the blunt head of diameter 92 mm, length 186 mm, and mass 5 kg was also created to study the effect of axial impact. The projectile was modelled as analytic rigid and the circular tubes as the deformable body. The moment of inertia and mass were ascribed at the center of gravity of the impactor. The impact velocities (range 33-83 m/s) were assigned on a reference point located at the center of gravity of the impactor in a predefined field module of ABAQUS/Explicit solver. The tubes were modelled using 4-node reduced integration quadrilateral 'S_4R' shell elements. The boundary conditions in the circular tube were assigned as fixed or 'Encastre' at the rear peripheral boundary of the tube. The contact between the circular tube and the cylindrical impactor was assigned using the penalty contact algorithm using a coefficient of friction 0.05. Three-dimensional numerical models are presented in Fig. 1.

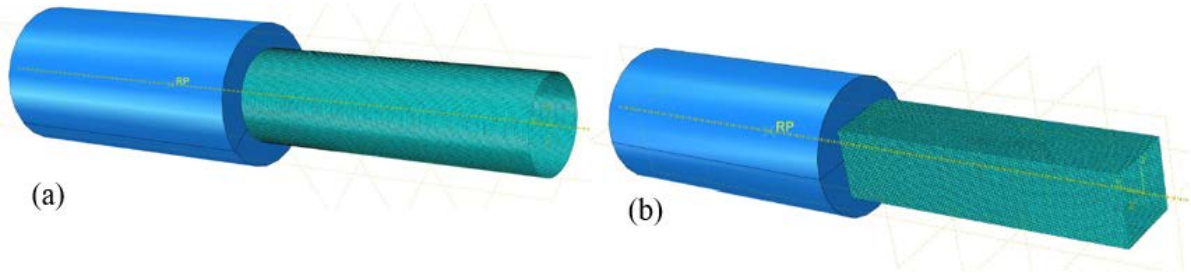

Fig. 1. 3 D model of (a) Projectile and circular tube and (b) Projectile and square tube

A mesh convergence analysis was carried out in order to obtain the optimum element size in the tubes. The maximum axial compression in tubes was observed numerically by increasing the number of elements in circular tubes of 60 mm diameter under the axial impact of 5 kg projectile with a constant velocity of 36.03 m/s. The element size of shell element 'S_4R' with unity aspect ratio was varied as 3, 2.5, 2, 1.5, 1.2, 1.0, 0.9, and 0.8 corresponding to the number of elements in between 4355 to 59239. It was found that maximum axial compression was increased linearly up to an element size of 1.2 mm×1.2 mm. However, further reducing the element size had a very insignificant effect on the results. Thus, the element size of 1.0 mm×1.0 mm was adopted for all tubes throughout the numerical models of this study. The Mesh convergence study is presented in Fig. 2.

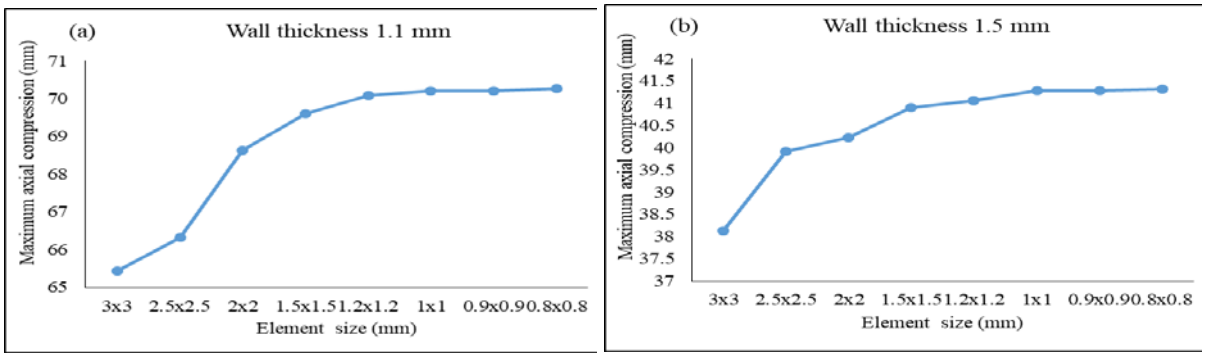

Fig. 2. Mesh convergence study of 60 mm diameter circular tube with wall thickness (a) 1.1 mm and (b) 1.5 mm under the axial impact of 5 kg projectile at 36.03 m/s velocity

3. Johnson-Cook constitutive material model

Johnson-Cook constitutive material model was used to define the material behavior of mild steel tubes to incorporate in numerical simulations. This model describes the behavior of

metals at high strain rates, large strains, and high temperatures [24-25]. The equivalent Von-Mises stress $\bar{\sigma}$ of the Johnson-Cook model is defined as:

$$\bar{\sigma}\left(\bar{\varepsilon}^{\mathrm{pl}}, \dot{\bar{\varepsilon}}^{\mathrm{pl}}, \hat{\mathrm{T}}\right) = \left[\mathrm{A} + \mathrm{B}\left(\bar{\varepsilon}^{\mathrm{pl}}\right)^{\mathrm{n}}\right]\left[1 + \mathrm{Cln}\left(\frac{\dot{\bar{\varepsilon}}^{\mathrm{pl}}}{\dot{\varepsilon}_0}\right)\right]\left[1 - \hat{\mathrm{T}}^{\mathrm{m}}\right], \tag{1}$$

where, $\dot{\varepsilon}_0$ is reference strain rate, $\bar{\varepsilon}^{\mathrm{pl}}$ is equivalent plastic strain, $\dot{\bar{\varepsilon}}^{\mathrm{pl}}$ is equivalent plastic strain rate, A, B, C, n, and m are material parameters obtained from various experiments and $\hat{\mathrm{T}}$ is related to temperature defined as:

$$\hat{\mathrm{T}} = (\mathrm{T} - \mathrm{T}_0)/(\mathrm{T}_{\mathrm{melt}} - \mathrm{T}_0), \quad \mathrm{T}_0 \le \mathrm{T} \le \mathrm{T}_{\mathrm{melt}}, \tag{2}$$

where T is the current temperature, T_0 is room temperature and $\mathrm{T}_{\mathrm{melt}}$ is designated as melting point temperature and the fracture model given by Johnson-Cook [25] includes the effect of temperature, strain rate, strain path, and stress-triaxiality on the equivalent fracture strain. The damage criterion is based on the damage development wherein the failure of the material is supposed to occur when the damage parameter D, exceeds unity.

$$D(\bar{\varepsilon}^{P}, \dot{\bar{\varepsilon}}^{P}, T, \sigma^{*}) = \sum \frac{\Delta\bar{\varepsilon}^{P}}{\bar{\varepsilon}_f^{\,P}(\dot{\bar{\varepsilon}}^{P}, T, \sigma^{*})}, \tag{3}$$

where $\bar{\varepsilon}_f^{\,P}$ is the plastic strain at failure and $\Delta\bar{\varepsilon}^{P}$ is an increment of the equivalent plastic strain. The equivalent fracture strain $\bar{\varepsilon}_{\mathrm{f}}^{\mathrm{pl}}$ is expressed as

$$\bar{\varepsilon}_{\mathrm{f}}^{\mathrm{pl}}\left(\frac{\sigma_m}{\bar{\sigma}}, \dot{\bar{\varepsilon}}^{\mathrm{pl}}, \hat{\mathrm{T}}\right) = \left[\mathrm{D}_1 + \mathrm{D}_2\exp\left(\mathrm{D}_3\frac{\sigma_{\mathrm{m}}}{\bar{\sigma}}\right)\right]\left[1 + \mathrm{D}_4\ln\left(\frac{\dot{\bar{\varepsilon}}^{\mathrm{pl}}}{\dot{\varepsilon}_0}\right)\right]\left[1 + \mathrm{D}_5\hat{\mathrm{T}}\right], \tag{4}$$

where, $\frac{\sigma_{\mathrm{m}}}{\bar{\sigma}}$ is the stress triaxiality ratio, σ_{m} is the mean stress and $\mathrm{D}_1 - \mathrm{D}_5$ are material parameters achieved from different mechanical tests. The material parameters used in the present investigation are given in Table 1 [26].

Table 1. Material parameter for mild steel [26]

Description	Notation	Numerical Value
Modulus of elasticity	E (N/m^2)	203×10^9
Poisson's ratio	v	0.33
Density	ρ (Kg/m^3)	7850
Yield stress constant	A (N/m^2)	304.330×10^6
Strain hardening constant	B (N/m^2)	422.007×10^6
	n	0.345
Viscous effect	C	0.0156
Thermal softening constant	m	0.87
Reference strain rate	$\dot{\varepsilon}_0$	0.0001 s^{-1}
Melting temperature	θ_{melt} (K)	1800
Transition temperature	$\theta_{transition}$ (K)	293
Fracture strain constant	D_1	0.1152
	D_2	1.0116
	D_3	-1.7684
	D_4	-0.05279
	D_5	0.5262

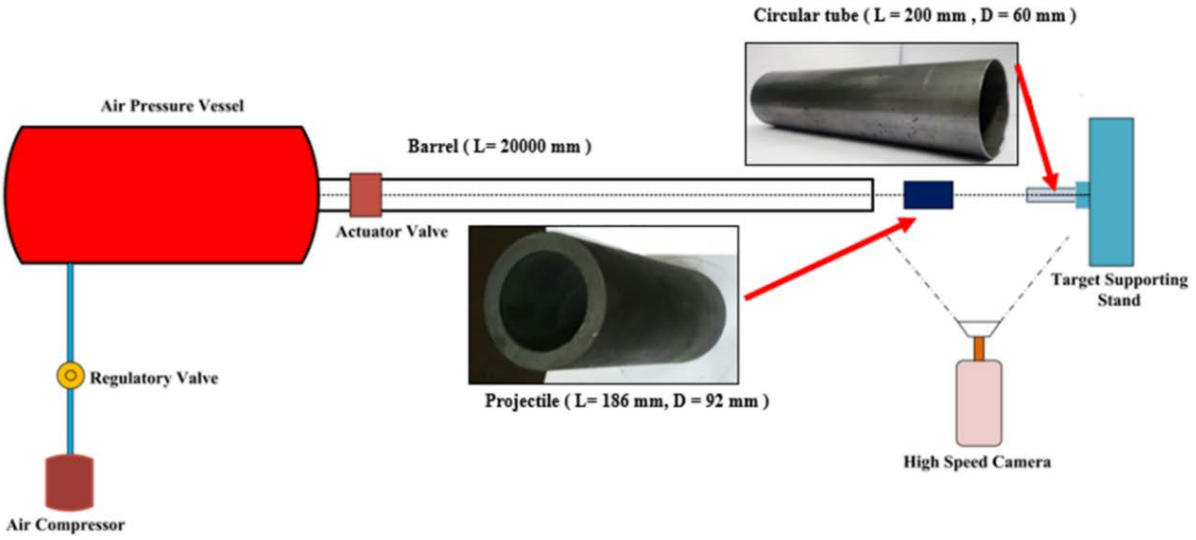

Fig. 3. Schematic of experimental setup

4. Results and discussion

The finite element computations were performed to study the axial performance of mild steel tubes with circular and square sections subjected to axial impact. The influence of wall thickness on axial shortening and energy absorption during axial impact was explored. In the present study, the actual and predicted results described good corroboration in the case of the circular tube with a wall thickness of 1.1 mm. The experiments have been carried out for validation of the computational model under dynamic impact conditions. Each specimen of 200 mm length was cut from a 6 m long hollow tube of 60 mm outer diameter and 1.1 mm wall thickness. The mild steel tubes were axially impacted by 5 kg hardened steel projectile (see Fig. 3). The axial deformation and energy absorption behavior of the tubes have been studied at different impact velocities in the range, 33-83 m/s. The experimental setup has been designed in such a manner that the projectile causes a precise axial deformation of the circular tube, see Fig. 3. The actual and predicted results with respect to the maximum axial deformation (compression) obtained corresponding to different velocities have been presented in Table 2 and Fig. 4.

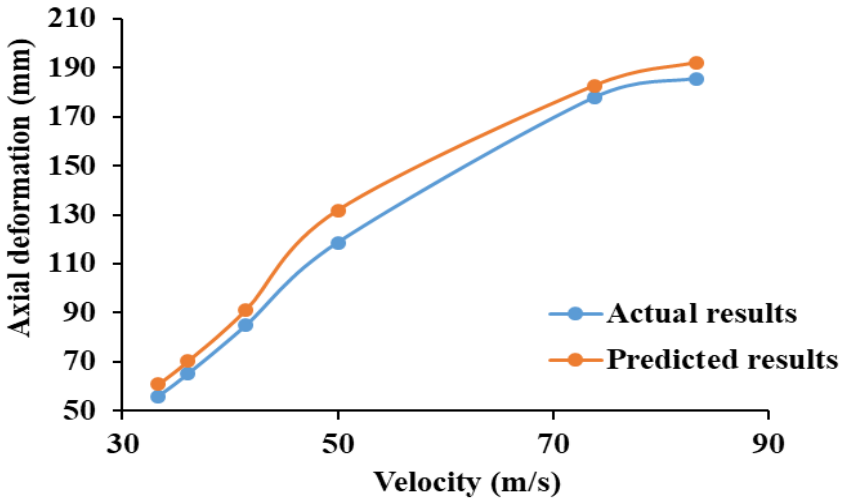

Fig. 4. Validation of numerical model

Table 2. Validation of the numerical model for the axial impact response of circular tubes

Test No.	Length of tube with dimensional tolerance (mm)	Diameter of tube with dimensional tolerance (mm)	Thickness of tube with dimensional tolerance (mm)	Mass of projectile (kg)	Velocity of projectile (m/s)	Impact energy (kJ)	Maximum axial deformation (mm)	
							Experimental study	Numerical study
60CC1	201.0±0.03	60.20±0.08	1.09±0.08	5	33.33	2777.22	56.0	60.87
60CC2	200.0±0.06	60.00±0.02	1.10±0.03	5	36.03	3245.4	65.0	70.2
60CC3	199.2±0.08	59.66±0.07	1.12±0.04	5	41.44	4293.18	84.83	91.13
60CC4	199.6±0.04	60.04±0.02	1.11±0.07	5	50.0	6250.0	118.67	131.81
60CC5	200.0±0.08	60.00±0.04	1.10±0.05	5	73.87	13641.94	177.77	182.56
60CC6	200.2±0.04	60.10±0.08	1.08±0.07	5	83.33	17359.72	185.60	192.84

A close correlation has been found between the experimental and numerical simulation results. A typical progressive deformation of 60 mm circular tube (against 36 m/s impact velocity) was captured by a high-speed camera, describing a close correspondence with its numerical simulation reproduction, see Fig. 5. The experimental and numerical simulation results for maximum axial deformation of 60 mm diameter tube were 65 and 70.2 mm, respectively, at 36 m/s velocity. At low impact velocities, the tubes experienced axisymmetric modes of plastic deformation, see Fig. 6(a) and (b). However, at higher incidence velocities, the tubes initially underwent concertina mode of plastic deformation which transformed into the diamond mode at the advanced stage of axial shortening, see Fig. 6(c) and (d), respectively. The actual and predicted maximum axial deformation of 60 mm circular tube were 177.77 mm and 182.56 mm respectively, at 73.87 m/s impact velocity.

The results of the maximum axial shortening and energy absorption for different wall thicknesses (1.1, 1.5, 2.0, 2.5, and 3.0 mm) of 60 mm circular tubes under axial impact with different velocities are presented in Table 3 and Fig. 7. The numerical deformation shapes of circular tubes of 60 mm diameter with different wall thicknesses under axial impact by 5 kg projectile at 41.44 m/s velocity are presented in Fig. 9. Axial compression in circular tubes was found to increase with an increase in the incidence velocity as shown in Table 3 and Fig. 7. By comparing axial compression of circular tubes of the reported five wall thicknesses, it was observed that the maximum axial deformation of circular tubes decreases with an increase in the wall thickness which is a resultant of the increased stiffness of the tube. The energy absorption of circular tubes did not vary significantly with an increase in wall thickness, however, it can be noted from Fig. 7 that energy absorption increases linearly with the increase in velocity irrespective of wall thickness. Similarly, maximum axial deformation and energy absorption for different wall thicknesses of 47.34 mm square tubes were compared in Table 4 and Fig. 8. The maximum axial deformation for square tubes has been found to increase with the increase in the incidence velocity of the projectile [22]. The rate of increase of axial deformation was higher in the thinner size square tube, see Table 4.

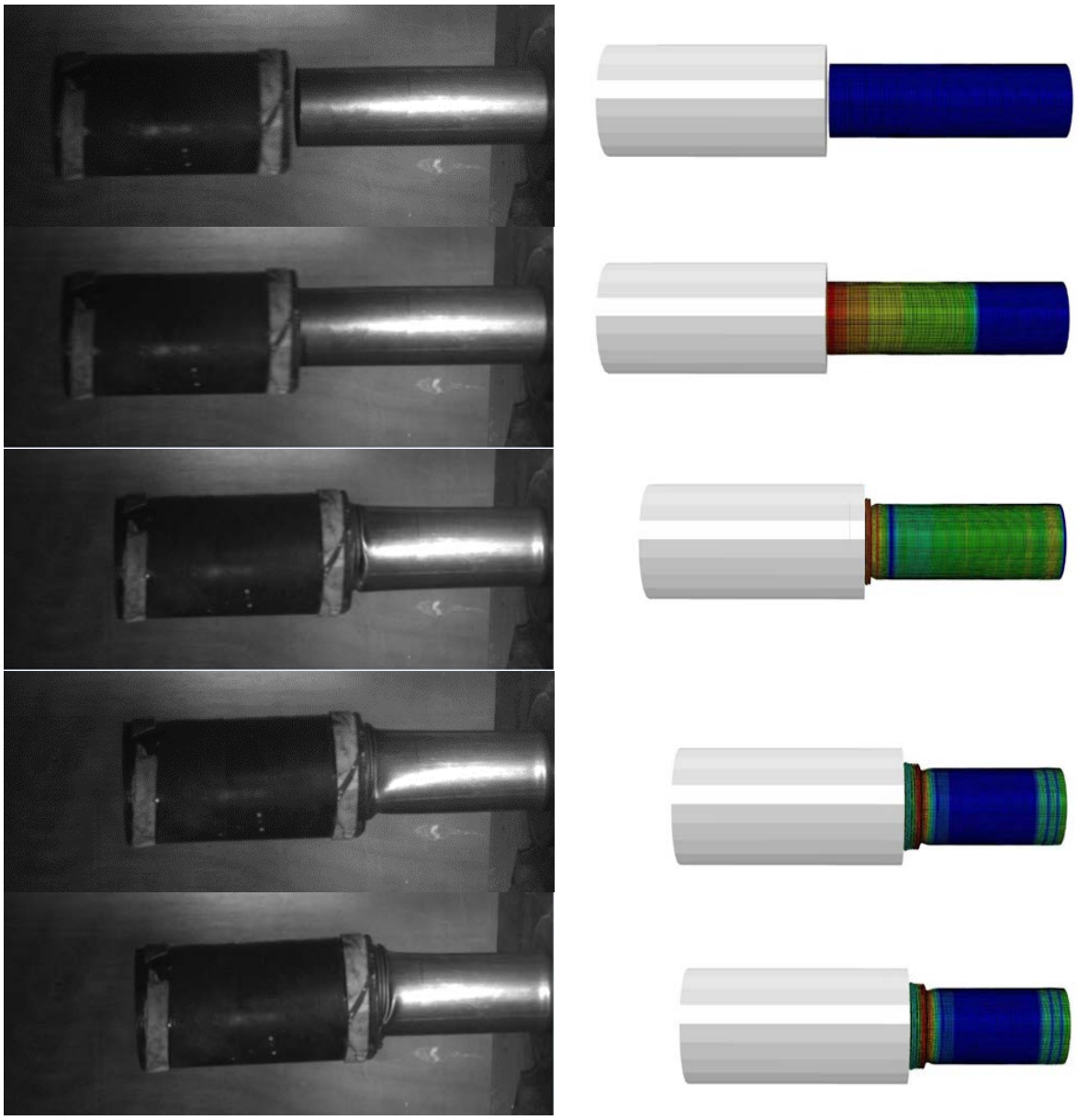

Fig. 5. Actual and predicted progressive deformation of 60 mm diameter tube under the axial impact of 5 kg projectile at 36 m/s incidence velocity

Table 3. Maximum axial deformation and energy absorption in the 60 mm circular tube of wall thickness 1.1, 1.5, 2, 2.5, and 3 mm impacted axially by 5 kg projectile

Velocity (m/s)	Maximum axial deformation in 60 mm circular tube (mm)					Energy absorption in 60 mm circular tube (Joule)				
	1.1 mm	1.5 mm	2.0 mm	2.5 mm	3.0 mm	1.1 mm	1.5 mm	2.0 mm	2.5 mm	3.0 mm
33.33	60.25	34.76	26.28	18.74	9.72	2772.89	2763.89	2756.93	2754.9	2724.4
36.03	70.20	41.29	28.21	25.30	11.35	3239.03	3233.92	3224.81	3219	3199.1
41.44	93.18	54.84	34.02	30.11	25.31	4286.05	4285.38	4279.44	4272	4253.9
50.0	132.6	80.42	50.46	36.96	33.91	6240.36	6234.32	6230.27	6229.2	6216.1
60.0	176.3	116.2	74.81	52.10	40.63	8996.88	8986.06	8984.53	8975.6	8969.1
65.0	179.3	136.3	87.72	62.35	46.90	10557.3	10552.8	10548.4	10542	10539
73.87	182.6	172.7	113.32	80.77	60.47	13638.4	13632.7	13625.3	13611	13607
83.33	192.0	182.5	141.56	102.19	77.53	17357.2	17349.5	17338.9	17337	17323

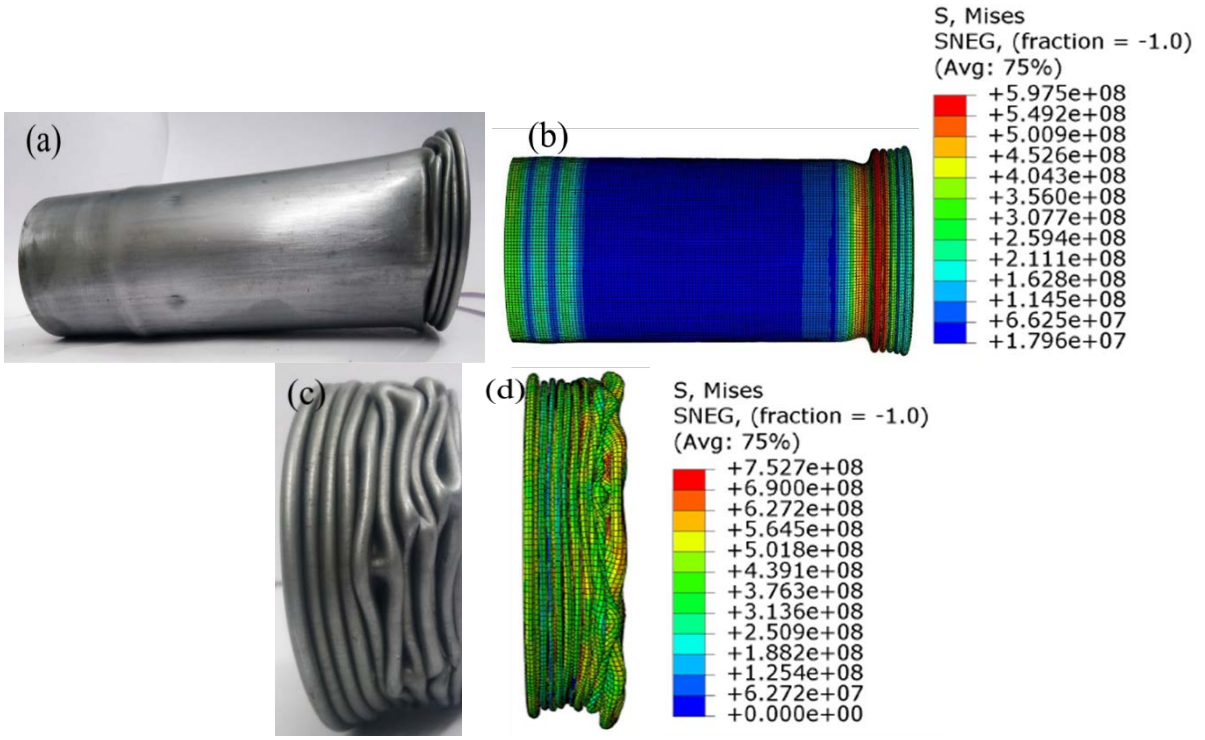

Fig. 6. Maximum axial deformation in 60 mm diameter tube (a) actual and (b) predicted at 36 m/s impact velocity and (c) actual and (d) predicted at 73.87 m/s impact velocity

Table 4. Maximum axial deformation and energy absorption in the 47.34 mm square tube of wall thickness 1.1, 1.5, 2, 2.5, and 3 mm impacted axially by 5 kg projectile

Velocity (m/s)	Maximum axial deformation in mild steel (mm)					Energy absorption in mild steel tube (Joule)				
	1.1 mm	1.5 mm	2.0 mm	2.5 mm	3.0 mm	1.1 mm	1.5 mm	2.0 mm	2.5 mm	3.0 mm
33.33	63.27	35.60	18.03	11.70	9.06	2767.5	2761.7	2756.3	2745	2718.6
36.03	76.02	42.05	22.61	13.84	10.20	3235.7	3230	3222.6	3215.7	3190.6
41.44	104.1	55.78	32.45	19.28	14.28	4282.8	4280.8	4276.9	4268.5	4248.6
50.0	159.9	82.01	47.94	32.17	21.46	6237.8	6230.7	6225.5	6222.7	6212.2
60.0	187.8	122.4	69.57	51.03	33.72	8985.7	8984.3	8979.4	8971.5	8967.5
65.0	190.1	147.3	84.85	57.13	42.18	10550	10544	10537	10532	10529
73.87	193.3	181.5	112.4	78.12	58.13	13624	13609	13606	13596	13579
83.33	195.3	192.3	136.9	94.95	75.45	17349	17339	17334	17333	17316

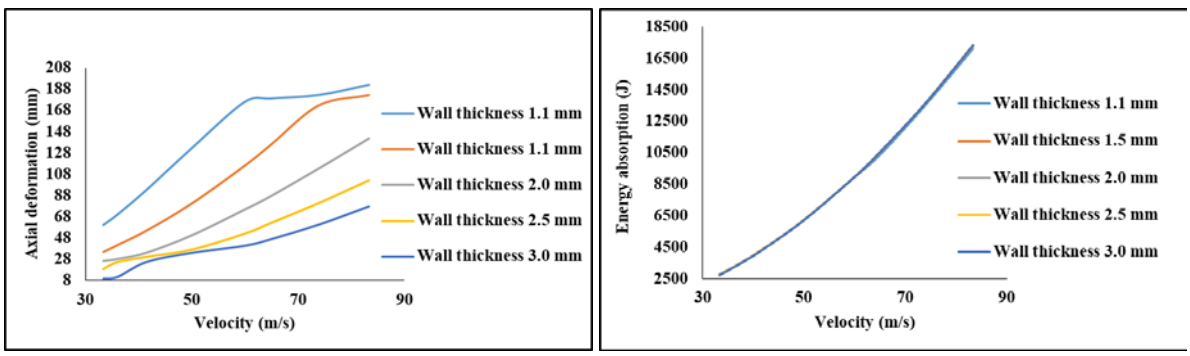

Fig. 7. Influence of wall thickness on axial deformation and energy absorption in a circular tube

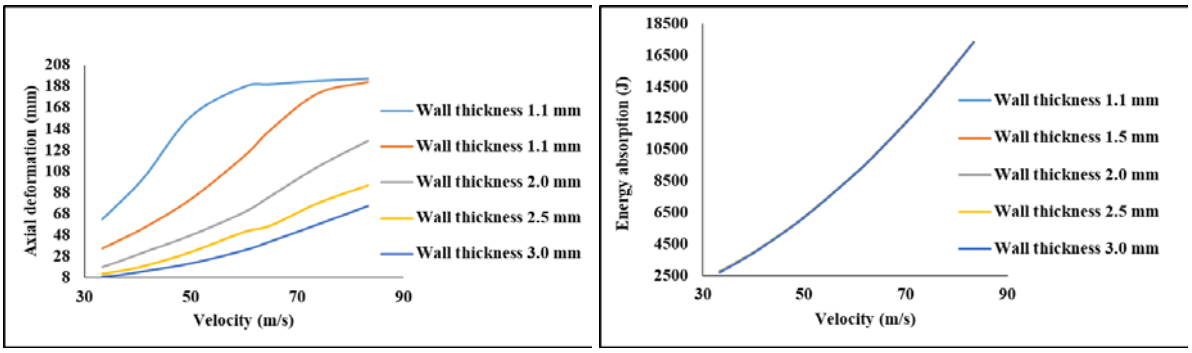

Fig. 8. Influence of wall thickness on axial deformation and energy absorption in square tube

The final axial compression of square tubes has been found to decrease with the increase in thickness due to the increased stiffness. It was found that thickness increase may be considered as a potential method to improve the impact resistance of the hollow tubes. The absorbed energy, on the other hand, did not show any significant influence on the wall thickness of the square tube. From Fig. 8, it can be observed that irrespective of the wall thickness of the tube, energy absorption increases linearly with the increase in velocity. Numerical deformation shapes of 60 mm diameter circular tubes with different wall thicknesses under axial impact by 5 kg projectile at 41.44 m/s velocity have been provided in Fig. 9. Initially, axial compression was found near the impacted end of the circular tube and a considerable portion of the initial kinetic energy was absorbed in compression during the initial deformation phase [2]. The maximum deformation has occurred in the tube with 1.1 mm wall thickness. The number of folds is decreasing at the impacted end with an increase in wall thickness and final axial deformation is also decreasing. The contour of Von-Mises stress is also changing due to the decrease in axial shortening of tubes as presented in Fig. 9. The folding of the square tube with 1.1 mm wall thickness under axial impact occurred in a symmetric manner, see Fig. 10 (a). The axial shortening of the thinner size tube has occurred at a faster rate and the final deformation is also higher. It has been noticed that the buckling started near the rear end of the square tube as the thickness is increasing, see Fig. 10 (c)-(e). However, at the initial stages of deformation, the first fold was formed at the impacted end of the tube with a radially outward buckle, see Fig. 10 (b). The buckling profile of equivalent circular and square tube sections with 1.1 mm wall thickness has been compared under the axial impact of 5 kg projectile at 83.33 m/s velocity in Fig. 11. Initially, the concertina mode of deformation was observed in circular tubes [3] and the diamond mode could also be noticed but due to full compression of the tube, the diamond formation could not be distinguished. However, the square tube buckled through symmetric progressive folding. For all tubes within the range simulated, the concertina collapse mode absorbs more energy than other deformation modes. This is because the energy absorption mostly depends on the amount of plastic deformation which takes place under axial loading.

(a) Wall thickness 1.1mm, Axial deformation =93.18 mm

(b) Wall thickness 1.5 mm, Axial deformation =54.84 mm

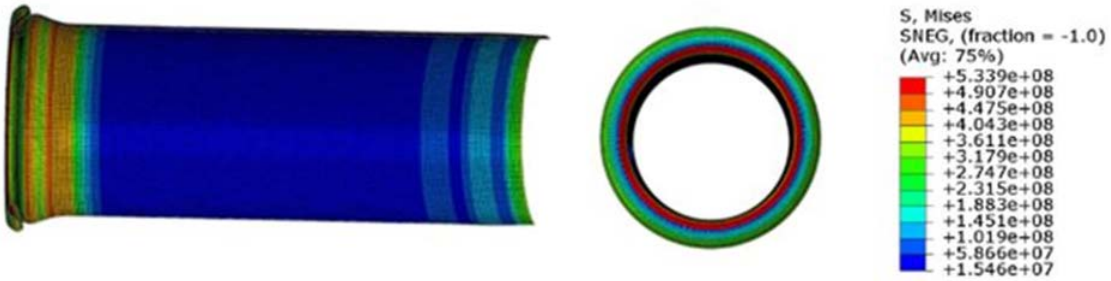

(c) Wall thickness 2 mm, Axial deformation =34.02 mm

(d) Wall thickness 2.5 mm, Axial deformation =30.11 mm

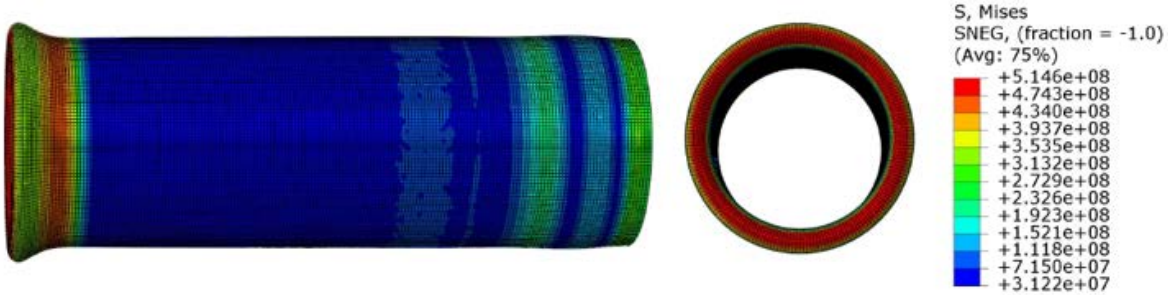

(e) Wall thickness 3 mm, Axial deformation = 25.31 mm

Fig. 9. Numerical deformation shapes and location of different Von-Mises stresses developed in circular tubes of 60 mm diameter with wall thickness (a) 1.1 mm, (b) 1.5 mm, (c) 2 mm, (d) 2.5 mm and (e) 3 mm under axial impact by 5 kg projectile at 41.44 m/s velocity

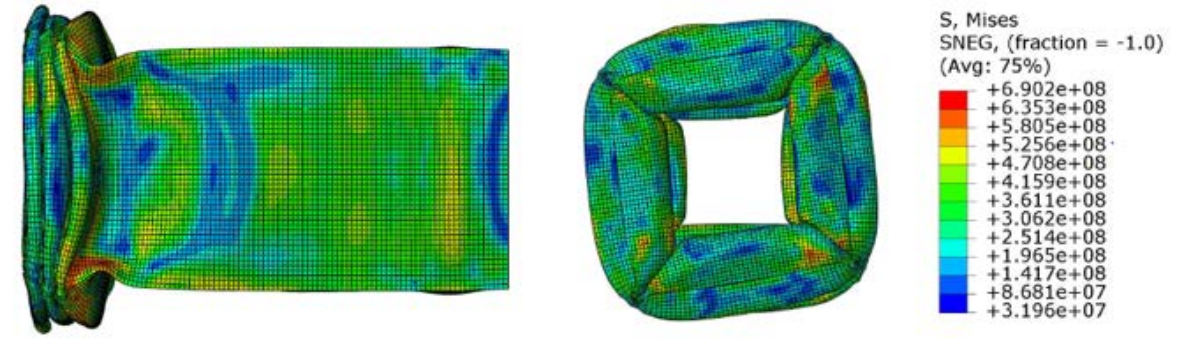

(a) Wall thickness 1.1 mm, Axial deformation = 104.1 mm

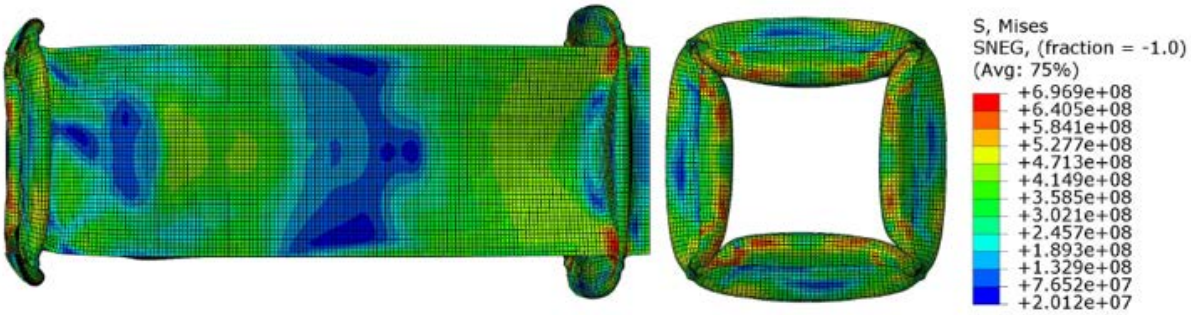

(b) Wall thickness 1.5 mm, Axial deformation = 55.78 mm

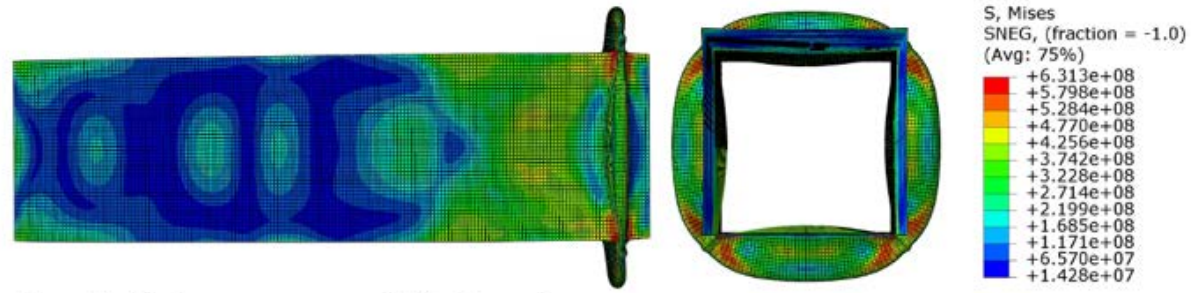

(c) Wall thickness 2 mm, Axial deformation = 32.45 mm

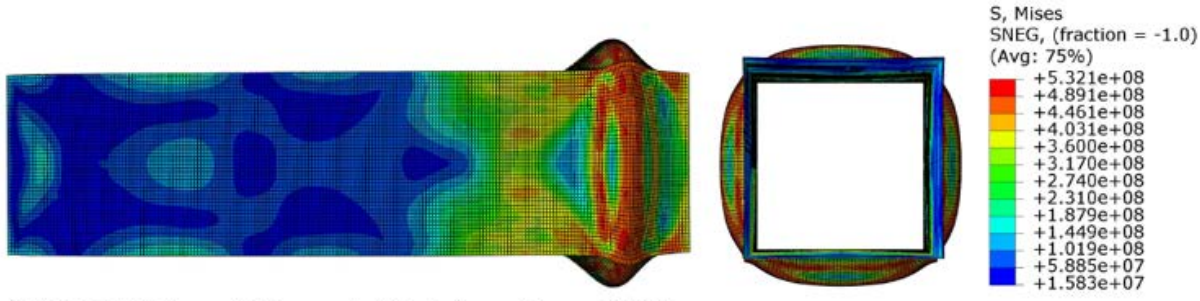

(d) Wall thickness 2.5 mm, Axial deformation = 19.28 mm

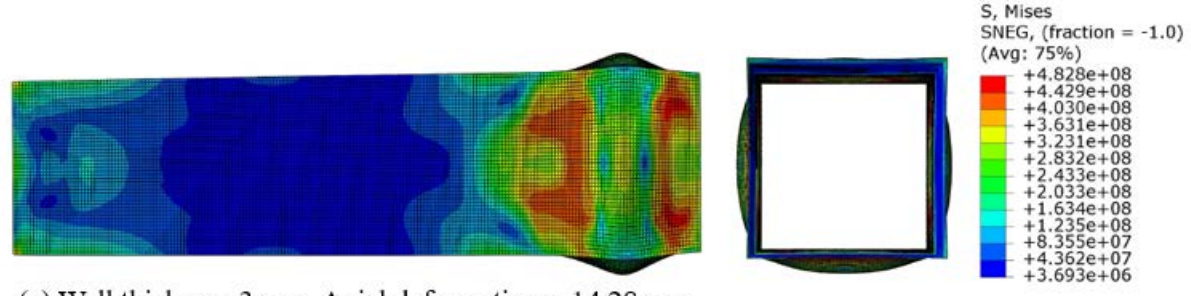

(e) Wall thickness 3 mm, Axial deformation = 14.28 mm

Fig. 10. Numerical deformation shapes and location of different Von-Mises stresses developed in square tubes of 47.34 mm with wall thickness (a) 1.1 mm, (b) 1.5 mm, (c) 2 mm, (d) 2.5 mm and (e) 3 mm under axial impact by 5 kg projectile at 41.44 m/s velocity

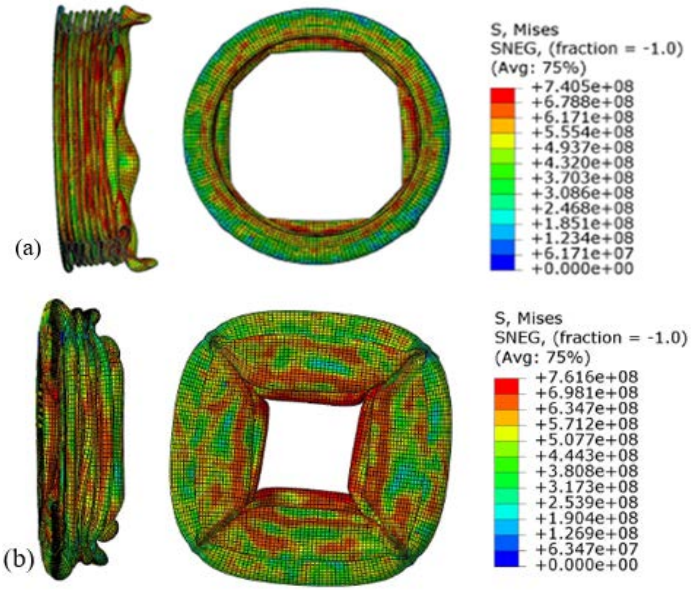

Fig. 11. Numerical deformation shapes and location of different Von-Mises stresses developed in (a) 60 mm circular tubes and (b) 47.34 mm square tubes with wall thickness 1.1 mm under axial impact by 5 kg projectile at 83.33 m/s velocity

Final axial deformation and energy absorption results for equivalent square and circular tube sections under axial impact with different velocities are presented in Tables 5-6. A comparative study has also been carried out on axial shortening and energy absorption behavior of circular and square tubes of the same equivalent section area with different thicknesses at the same impact energy under projectile impact. Under the axial impact of 5 kg projectile, the maximum axial compression of the square tubes was found to be higher for a given equivalent geometric section for 1.1 and 1.5 mm thicknesses [22], see Table 5. At higher thicknesses, on the other hand, the axial compression of the circular tubes was found higher. At low incidence velocities, this effect was more prominent, and it diminished at the higher incidence velocities. On the other hand, the energy absorption in the equivalent circular and square tube sections have been found to be almost the same for different wall thicknesses, Table 6.

Table 5. Comparison of maximum axial deformation of the equivalent circular and square tube sections with different wall thicknesses

Velocity (m/s)	Maximum axial deformation in mild steel tubes (mm)									
	1.1 mm		1.5 mm		2.0 mm		2.5 mm		3.0 mm	
	60 mm circular tube	47.34 mm square tube	60 mm circular tube	47.34 mm square tube	60 mm circular tube	47.34 mm square tube	60 mm circular tube	47.34 mm square tube	60 mm circular tube	47.34 mm square tube
33.33	60.25	63.27	34.76	35.60	26.28	18.03	18.74	11.70	9.72	9.06
36.03	70.20	76.02	41.29	42.05	28.21	22.61	25.30	13.84	11.35	10.20
41.44	93.18	104.1	54.84	55.78	34.02	32.45	30.11	19.28	25.31	14.28
50.0	132.6	159.9	80.42	82.01	50.46	47.94	36.96	32.17	33.91	21.46
60.0	176.3	187.8	116.2	122.4	74.81	69.57	52.10	51.03	40.63	33.72
65.0	179.3	190.1	136.3	147.3	87.72	84.85	62.35	57.13	46.90	42.18
73.87	182.6	193.3	172.7	181.5	113.32	112.4	80.77	78.12	60.47	58.13
83.33	192.0	195.3	182.5	192.3	141.56	136.9	102.19	94.95	77.53	75.45

Table 6. Comparison of energy absorption of the equivalent circular and square tube sections with different wall thicknesses

Velocity (m/s)	Energy absorption by mild steel tubes (Joule)									
	1.1 mm		1.5 mm		2.0 mm		2.5 mm		3.0 mm	
	60 mm circular tube	47.34 mm square tube	60 mm circular tube	47.34 mm square tube	60 mm circular tube	47.34 mm square tube	60 mm circular tube	47.34 mm square tube	60 mm circular tube	47.34 mm square tube
33.33	2772.89	2767.5	2763.89	2761.7	2756.93	2756.3	2754.9	2745	2724.4	2718.6
36.03	3239.03	3235.7	3233.92	3230	3224.81	3222.6	3219	3215.7	3199.1	3190.6
41.44	4286.05	4282.8	4285.38	4280.8	4279.44	4276.9	4272	4268.5	4253.9	4248.6
50.0	6240.36	6237.8	6234.32	6230.7	6230.27	6225.5	6229.2	6222.7	6216.1	6212.2
60.0	8996.88	8985.7	8986.06	8984.3	8984.53	8979.4	8975.6	8971.5	8969.1	8967.5
65.0	10557.3	10550	10552.8	10544	10548.4	10537	10542	10532	10539	10529
73.87	13638.4	13624	13632.7	13609	13625.3	13606	13611	13596	13607	13579
83.33	17357.2	17349	17349.5	17339	17338.9	17334	17337	17333	17323	17316

5. Conclusions

The finite element computations were performed to study the influence of thickness on axial deformation and energy absorption behavior of the circular and square tubes with equivalent section area under dynamic impact. The experiments have been carried out under axial impact of 5 kg projectile for validation of the constitutive and computational model. The actual and predicted axial compression in the circular tubes are closely validated. A comparative study of the equivalent circular and square tube sections with respect to axial compression and energy absorption has also been carried out at different wall thicknesses. The maximum axial deformation of both tubes has been found to increase with the increase in the impact velocity of the projectile. Due to the axial impact of the projectile, the axial deformation of circular and square tubes decreased with an increase in the wall thickness due to the increased stiffness of the tube. However, the energy absorption of circular and square tubes did not vary significantly with the change of wall thickness of the tube. It was observed that the maximum axial deformation of the square tubes was higher than equivalent circular tubes of 1.1 and 1.5 mm thickness. At higher thicknesses, the axial compression of the circular tubes was found higher than the square tube. The absorbed energy did not show any significant effect of the equivalent circular and square tube sections with different wall thicknesses. The concertina mode of folding was observed in circular tubes at the initial stage which transformed into diamond mode at higher impact velocities and the symmetric progressive folding was found in the square tube.

References

[1] Rajabiehfard R, Darvizeh A, Alitavoli M, Sadeghi H, Noorzadeh N, Maghdouri E. Experimental and numerical investigation of dynamic plastic behavior of tube with different thickness distribution under axial impact. *Thin-Walled Structures.* 2016;109: 174-184.

[2] Karagiozova D, Jones N. Dynamic elastic–plastic buckling of circular cylindrical shells under axial impact. *International Journal of solids and Structures.* 2000;37(14): 2005-2034.

[3] Nia AA, Hamedani JH. Comparative analysis of energy absorption and deformations of thin walled tubes with various section geometries. *Thin-Walled Structures.* 20101;48(12): 946-954.

[4] Zhang X, Zhang H, Wen Z. Axial crushing of tapered circular tubes with graded thickness. *International Journal of Mechanical Sciences.* 2015;92: 12-23.

[5] Xu F. Enhancing material efficiency of energy absorbers through graded thickness structures. *Thin-Walled Structures.* 2015;97: 250-265.
[6] Zhang H, Zhang X. Crashworthiness performance of conical tubes with nonlinear thickness distribution. *Thin-Walled Structures.* 2016;99: 35-44.
[7] Nikkhah H, Baroutaji A, Olabi AG. Crashworthiness design and optimisation of windowed tubes under axial impact loading. *Thin-Walled Structures.* 2019;142: 132-148.
[8] Tran T. Crushing analysis under multiple impact loading cases for multi-cell triangular tubes. *Thin-Walled Structures.* 2017;113: 262-272.
[9] Manaf EH, Rahman MT, Syayuthi AR, Mat F, Rahman A. Crashworthiness analysis of empty singular aluminium tubes with varying shapes in LS-Dyna. *AIP Conference Proceedings.* 2018;2030(1): 020115.
[10] Zahran MS, Xue P, Esa MS. Novel approach for design of 3D-multi-cell thin-walled circular tube to improve the energy absorption characteristics under axial impact loading. *International Journal of Crashworthiness.* 2017;22(3): 294-306
[11] Rahi A. Controlling energy absorption capacity of combined bitubular tubes under axial loading. *Thin-Walled Structures.* 2018;123: 222-231.
[12] Vinayagar K, Kumar AS. Crashworthiness analysis of double section bi-tubular thin-walled structures. *Thin-Walled Structures.* 2017;112: 184-193.
[13] Xie S, Yang W, Li H, Wang N. Impact characteristics and crashworthiness of multi-cell, square, thin-walled, structures under axial loads. *International Journal of Crashworthiness.* 2017;22(5): 503-517.
[14] Hao W, Xie J, Wang F. Theoretical prediction of the progressive buckling and energy absorption of the sinusoidal corrugated tube subjected to axial crushing. *Computers & Structures.* 2017;191: 12-21.
[15] Liu Z, Hao W, Xie J, Lu J, Huang R, Wang Z. Axial-impact buckling modes and energy absorption properties of thin-walled corrugated tubes with sinusoidal patterns. *Thin-Walled Structures.* 2015;94: 410-423.
[16] Isaac CW, Oluwole O. Energy absorption improvement of circular tubes with externally press-fitted ring around tube surface subjected under axial and oblique impact loading. *Thin-Walled Structures.* 2016;109: 352-366.
[17] Wei Y, Yang Z, Yan H, Guo Y, Wu X, Huang C. Proactive regulation of axial crushing behavior of thin-walled circular tube by gradient grooves. *International Journal of Mechanical Sciences.* 2016;108: 49-60.
[18] Azimi MB, Asgari M. A new bi-tubular conical–circular structure for improving crushing behavior under axial and oblique impacts. *International journal of mechanical sciences.* 2016;105: 253-265.
[19] Nia AA, Chahardoli S. Mechanical behavior of nested multi-tubular structures under quasi-static axial load. *Thin-Walled Structures.* 2016;106: 376-389.
[20] Estrada Q, Szwedowicz D, Rodriguez-Mendez A, Elías-Espinosa M, Silva-Aceves J, Bedolla-Hernández J, Gómez-Vargas OA. Effect of radial clearance and holes as crush initiators on the crashworthiness performance of bi-tubular profiles. *Thin-Walled Structures.* 2019;140: 43-59.
[21] Deng X, Qin S, Huang J. Energy absorption characteristics of axially varying thickness lateral corrugated tubes under axial impact loading. *Thin-Walled Structures.* 2021;163: 107721.
[22] Tak SK, Iqbal MA. Axial compression behaviour of thin-walled metallic tubes under quasi-static and dynamic loading. *Thin-Walled Structures.* 2021;159: 107261.
[23] Baroutaji A, Sajjia M, Olabi AG. On the crashworthiness performance of thin-walled energy absorbers: recent advances and future developments. *Thin-Walled Structures.* 2017;118: 137-163.

[24] Johnson GR, Cook WH. A constitutive model and data for metals subjected to large strains, high strain rates and high temperatures. In: *Proceedings of the 7th International Symposium on Ballistics.* 1983. p.541-547.
[25] Johnson GR, Cook WH. Fracture characteristics of three metals subjected to various strains, strain rates, temperatures and pressures. *Engineering fracture mechanics.* 1985;21(1): 31-48.
[26] Iqbal MA, Senthil K, Bhargava P, Gupta NK. The characterization and ballistic evaluation of mild steel. *International Journal of Impact Engineering*. 2015;78: 98-113.

THE AUTHORS

Tak S.K.
e-mail:sanjay.tak81@gmail.com
ORCID: 0000-0002-9417-1331

Iqbal M.A.
e-mail:ashraf.iqbal@ce.iitr.ac.in
ORCID:0000-1310-3939-0500